MRS Advances © 2018 Materials Research Society
DOI: 10.1557/adv.2018.586

Application of raw and modified Uruguayan clays to phosphate adsorption for water remediation

Pablo González[1], Andrea C. De Los Santos[2], Jorge R. Castiglioni[2], María A. De León[2,*]

[1]*Grupo de Instrumentación y Automatización en Química Analítica (GIAQA), Área Química Analítica, DEC, Facultad de Química, Universidad de la República, Montevideo, Uruguay.*
[2]*Laboratorio de Fisicoquímica de Superficies, DETEMA, Facultad de Química, Universidad de la República, Montevideo, Uruguay.*

ABSTRACT

A raw clay from Uruguay was modified with aluminium to obtain an aluminium pillared clay (Al-PILC). The solids were characterized by scanning electron microscopy, X-ray diffraction and nitrogen adsorption-desorption isotherms. The Al-PILC retained the typical laminar structure of montmorillonite. The specific surface area and the microporous volume of the Al-PILC, 235 m^2 g^{-1} and 0.096 cm^3 g^{-1}, respectively, were much higher than those of the clay. The phosphate adsorption capacity of the Al-PILC was higher than those of the clay. The phosphate adsorption kinetic followed the pseudo-first-order model for both, the clay and the Al-PILC, and the phosphate adsorption isotherm for the Al-PILC fit the Freundlich model.

INTRODUCTION

Phosphorus plays a fundamental role in the metabolism of plants and animals, being part of the main metabolic cycles of organisms. In environmental waters phosphorus control is essential since a high load of this element leads to the eutrophication of water courses; concentrations of phosphorus greater than 0.1 mg L^{-1} are enough to induce a proliferation of cyanobacteria [1]. High phosphorus loads may be due to the use of fertilizers in soils near watercourses, the use of detergents containing polyphosphates as additives, the use of phosphates in water treatments, etc. In the environment this element exists under diverse chemical forms but in the watercourses, phosphorus is found mostly as orthophosphates [2]. Therefore, the removal of phosphate from water represents a possible solution to the problem.

Several processes have been developed to eliminate phosphate in wastewater such as biologic treatments using phosphorus accumulating organisms, ion exchange,

chemical precipitation and adsorption. Among these processes, adsorption is one of the most promising due to its efficiency and simplicity. Different adsorbents have been used, for instance, mesoporous silica materials [3], resin [4] and clays [1,5,6]. Although relatively effective phosphate removals have been achieved, the development of effective and low-cost solid adsorbent is still a matter of study.

Clays are natural and abundant solids materials with laminar structures and high cation exchange capacity. They can be modified introducing voluminous polycations in the interlayer space which are transformed in oxidic species by calcination. This produces nanoporous materials with high specific surface area. These nanomaterials are known as pillared interlayered clays (PILCs) and are attractive as catalysts and adsorbents. Uruguay has a high-quality natural clay. Taking advantage of the existence of this cheap and available natural resource, the present work studies the use of this clay and the clay pillared with aluminum (Al-PILC) to the removal of phosphate from water by adsorption.

EXPERIMENTAL

A raw clay was extracted form Bañado de Medina, Uruguay. More than 80% of the clay is a calcium-rich montmorillonite with a low sodium and potassium content [7]. The raw clay was dried at 105 °C for 24 h, ground and sieved. The fraction with aggregates sizes less than 250 μm was selected and name as clay. An Al-polyhydroxycation intercalating solution was prepared by gradually adding a solution of NaOH (0.4 mol L^{-1}) over an $AlCl_3$ solution (1.0 mol L^{-1}), while vigorous stirring was kept, until a final molar ratio $OH^-/Al^{3+} = 2$ was obtained [7,8]. The resulting solution was aged for 1 h at 50 °C and added to an aqueous suspension of the clay (10% w/w). The volume of the intercalating solution was the necessary to achieve a ratio of 5 mmol of Al per gram of Clay. pH was adjusted to 5.5 with NaOH and the suspension was kept for 3 h at 80 °C and 16 h at room temperature [7,8]. The solid was separated by filtration, washed with deionized water, oven dry at 100 ^oC and calcined at 600 °C for 2 h. The resulting pillared clay was identified as Al-PILC.

Scanning electron microscopy (SEM) images were obtained with a JEOL JS M-5900LV scanning electron microscope operated at 20 kV. The powder X-ray diffraction data were obtained in a Rigaku Ultima IV powder diffractometer operating in Bragg Brentano geometry using Cu Kα radiation (0.15418 nm). Nitrogen adsorption-desorption isotherms were obtained at -196 °C in a Quantachrome, Autosorbe-1 equipment.

Experiments for the study of phosphate adsorption kinetic were performed in glass bottles suspending 0.5 g of clay or Al-PILC in 150 mL of KH_2PO_4 aqueous solution with an initial phosphorous concentration of 50 mg P L^{-1}. The closed bottles were place in an orbital shaker at 20 °C and 200 rpm and samples were taken at different times.

The batch adsorption experiments were performed in glass bottles. 0.13 g of Al-PILC were added in each one with 50 mL of KH_2PO_4 aqueous solution with different initial concentrations. The closed bottles were placed in an orbital shaker for 24 h at 20 °C and 200 rpm, and supernatant samples were taken at the end of the tests.

All the samples were immediately filtered, and phosphate concentration was determined spectrophotometrically by the Vanadomolybdophosphoric Acid Colorimetric Method (Standard Method 4500-P C) [10] using a UV-Vis spectrophotometer HP 8453.

RESULTS AND DISCUSSION

The morphology of the clay and the Al-PILC can be observed in the SEM images included in Figure 1. The laminar and well-ordered structure distinctive of the

flat particles of montmorillonite clays is evidenced in Figure 1.a. This image shows a dominant morphology in the form of flakes where only interparticle pores are appreciated. The micrograph in Figure 1.b. evidence that the Al-PILC retains the typical laminar structure of montmorillonite, even though partial swelling of the solid and increased structural disorder are observed. The Al-PILC has a porous appearance due to the increase of microporosity associated with the intercalation of aluminum oxide pillars in the interlayer space of the montmorillonite.

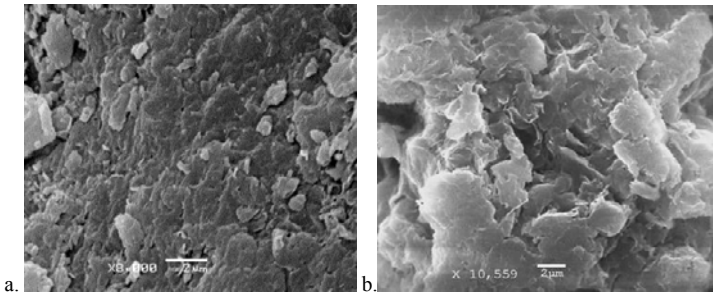

Figure 1. SEM micrograph of the solids: a) clay and b) Al-PILC.

Figure 2. shows the results of the X-ray diffraction analysis for the clay and the Al-PILC. The diffractogram for the clay shows a sharp peak at 5.95 ° corresponding to the d_{001} basal spacing of montmorillonite with a value of 1.48 nm. Peaks for quartz presented as impurities in the clay were also identified. A well-defined peak at $2\theta = 5.05°$ is detected for the Al-PILC which corresponds to a d_{001} value of 1.75 nm. This result confirm that the pillaring process generated a thermally stable basal spacing.

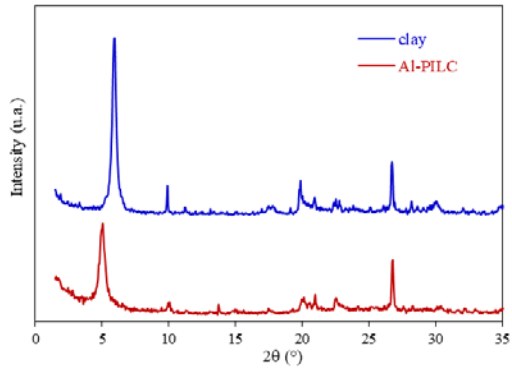

Figure 2. X-ray diffraction diagrams for the clay and the Al-PILC.

Figure 3 shows the nitrogen adsorption-desorption isotherm for the clay and the Al-PILC. The clay isotherm is Type II with a type H4 hysteresis cycle [9]. This behavior is distinctive of the presence of narrow pores between the flat montmorillonite particles. However, the Al-PILC isotherm shows significant adsorption at low relative pressures (Type I isotherm) and a small hysteresis cycle (Type IV isotherm) representative of the existence of micropores and mesopores, respectively [9].

Table I summarizes the textural properties derived from the nitrogen adsorption data: specific surface area (S_{BET}), specific micropore volume ($V_{\mu p}$) and specific total pore volume (V_T). The specific surface area and the microporous volume of the Al-PILC are much higher than those of the clay. These results confirm the efficiency of the pillaring process to generate a microporous structure in the clay by the incorporation of aluminium polyhydroxycations. Changes in textural properties could affect the type and number of active sites and thereby the phosphate adsorption.

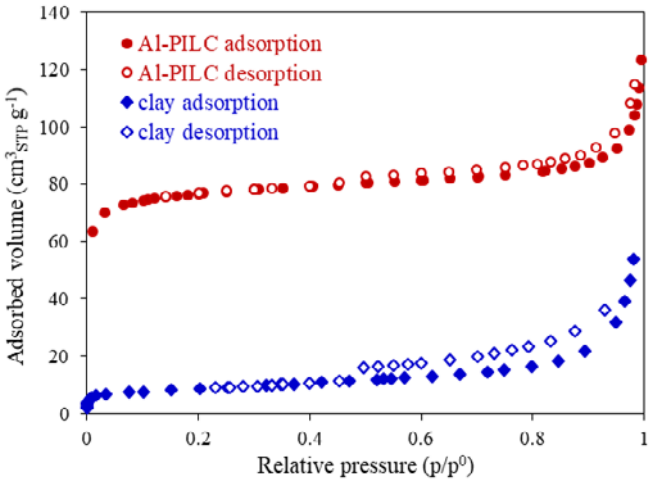

Figure 3. Nitrogen adsorption-desorption isotherms for the clay and the Al-PILC.

Table I. Textural properties of the clay and the Al-PILC.

Solid	S_{BET} (m^2 g^{-1})	V_T (cm^3 g^{-1})	$V_{\mu m}$ (cm^3 g^{-1})
Clay	29	0.047	0.012
Al-PILC	235	0.167	0.096

Figure 4 shows the results of phosphate adsorption kinetic experiments for the clay and the Al-PILC. Q_t (mg P g^{-1}) is the adsorption capacity determined for different contact times by Equation 1:

$$Q_t = \frac{(C_0 - C_t)\,V}{m} \qquad (1)$$

where C_0 (mg P L^{-1}) is the initial phosphate concentration, C_t (mg P L^{-1}) is the phosphate concentration at certain time t, V (L) is the phosphate solution volume and m (g) is the adsorbent mass. As can be seen in Figure 4, both solids show an increase in the

phosphate adsorption capacity by increasing the contact time and attain the adsorption equilibrium in about 24 h. However, the phosphate adsorption rate is comparatively higher for the Al-PILC. In addition, the equilibrium adsorption capacity (Q_{eq}) is higher for the Al-PILC, reaching a value of 8.31 mg P g^{-1}, 41% higher than that of the clay (5.89 mg P g^{-1}).

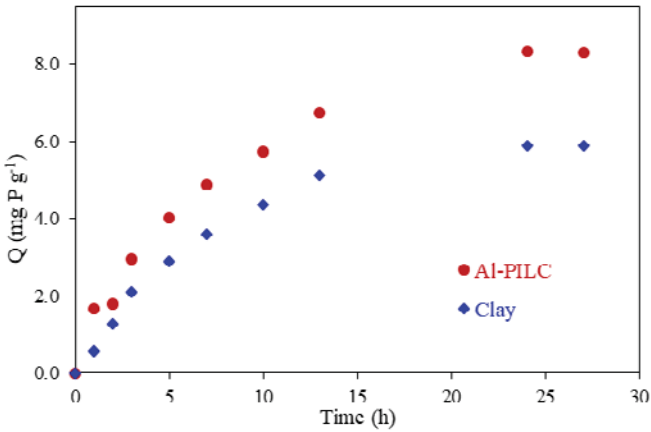

Figure 4. Phosphate adsorption on the clay and the Al-PILC as a function of contact time.

The phosphate adsorption kinetic data were fitted with the pseudo-first-order and pseudo-second-order kinetic models, Equations 2 and 3, respectively [1]:

$$\ln(Q_{eq} - Q_t) = lnQ_{eq} - k_1 t \qquad (2)$$

$$\frac{t}{Q_t} = \frac{1}{k_2 Q_{eq}^2} + \frac{1}{Q_{eq}}\, t \qquad (3)$$

where k_1 and k_2 are the pseudo-first-order and pseudo-second-order rate constants, respectively. These constants and the equilibrium adsorption capacity calculated from the kinetic models ($Q_{eq,cal}$) were determined from the linear plot of $ln(Q_{eq} - Q_t)$ vs. t for pseudo-first-order model and t/Q_t vs. t for pseudo-second-order model. The results as well as the correlation coefficients (R^2) are shown in Table II. The correlation coefficient for the pseudo-first order model is relatively higher than that of the pseudo-second-order for both adsorbents. Moreover, lower difference between the experimental and calculated equilibrium adsorption capacity is observed for the pseudo-first-order model. Therefore, it can be concluded that the pseudo-first-order model better explains the kinetics of phosphate adsorption on the clay and the Al-PILC.

Table II. Kinetic parameters for the phosphate adsorption on the clay and the Al-PILC.

	Pseudo-first-order			Pseudo-second-order		
	k_1 (h^{-1})	$Q_{eq,cal}$ (mg P g^{-1})	R^2	k_2 (g mgP^{-1} h^{-1})	$Q_{eq,cal}$ (mg P g^{-1})	R^2
Clay	0.150	6.18	0.9894	0.036	9.06	0.9580
Al-PILC	0.120	7.97	0.9917	0.019	11.03	0.9694

The phosphate adsorption isotherm for the Al-PILC is shown in Figure 5. The equilibrium adsorption capacity (Q_{eq}, mg P g^{-1}) was determined by the following equation:

$$Q_{eq} = \frac{(C_0 - C_{eq})\,V}{m} \qquad (4)$$

where C_{eq} is the equilibrium concentrations of phosphate in solution (mg P L^{-1}), and C_0, V and m have the same meaning as in Equation 1. Q_{eq} of the Al-PILC significantly increases with the equilibrium phosphate concentration in the low concentrations range. However, at high concentrations the increase in the amount adsorbed is slow due to the progressive occupation of the active sites of the solid. The maximum removal capacity of the Al-PILC was 48.7 mg P g^{-1} and was achieved with an equilibrium concentration of 275 mg P L^{-1}.

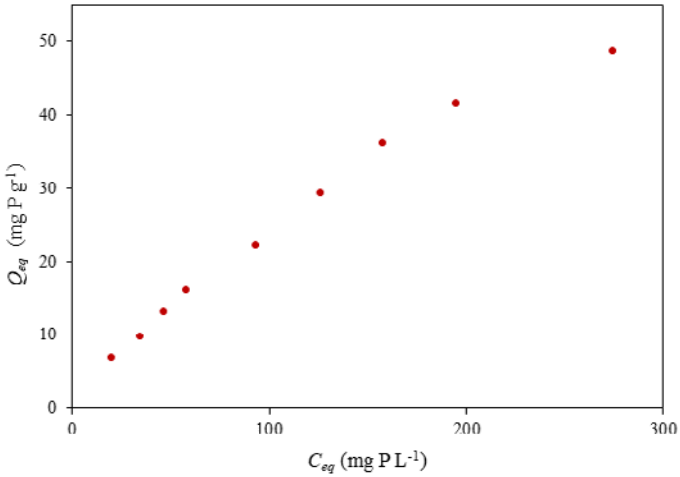

Figure 5. Phosphate adsorption isotherm for the Al-PILC.

The equilibrium adsorption data were correlated with Langmuir (Equation 5) and Freundlich (Equation 6) models:

$$Q_{eq} = \frac{Q_m K_L C_{eq}}{1 + K_L Ceq} \qquad (5)$$

$$Q_{eq} = K_F\, C_{eq}^{\frac{1}{n}} \qquad (6)$$

where K_L (L mg^{-1}) and Q_m (mg g^{-1}) are Langmuir constants, and K_F (mg g^{-1}) and n (dimensionless) are Freundlich constants. These parameters were determined from the slop and intercept of the linear plot of Q_{eq}/C_{eq} vs. C_{eq} for Langmuir model and ln Q_{eq} vs.

ln C_{eq} for Freundlich model. Table III shows the results and the correlation coefficients (R^2) obtained for each model. According to the correlation coefficients values, the experimental phosphate adsorption isotherm obtained for the Al-PILC presents a good fit to Freundlich adsorption model. This finding agrees with that observed by other authors in previous studies on the phosphate adsorption on clays [5] and Al-PILCs [11].

The mechanism of phosphate adsorption onto the clay and the Al-PILC can be complex. It has been suggested that the mechanism involved is a combination of physical and chemical processes, in which adsorption can be attributed to electrostatic attractions and chemical interactions [5,6].

Table III. Langmuir and Freundlich isotherm parameters for phosphate adsorption on the Al-PILC.

Langmuir			Freundlich		
Q_m (mg P g^{-1})	K_L (L mg^{-1})	R^2	K_F	$1/n$	R^2
109	3.01 x 10^{-3}	0.9407	0.656	0.780	0.9955

CONCLUSIONS

The raw clay as well as the Al-PILC showed phosphate adsorption capacity, but the Al-PILC showed a significantly greater capacity than the clay. Therefore, the modification of the clay with aluminium was efficient to improve its adsorption capacity. For both materials, the adsorption kinetics fits to a pseudo-first-order model and the phosphate adsorption for the Al-PILC follows the Freundlich model.

ACKNOWLEDGEMENTS

Authors thanks PEDECIBA-Química for the financial support and Dr. Ricardo Faccio (Cryssmat-Lab, Universidad de la República) for X-ray diffraction analysis.

REFERENCES

[1] L. Deng and Z. Shi, J. Alloys Comp. 637, 188 (2015).
[2] J. De Zuane, *Handbook of Drinking Water Quality*, 2nd ed. (Wiley, New York, 1997).
[3] J.D. Zhang, Z.M. Shen, W.P. Shan, Z.J. Mei and W.H. Wang, J. Hazard. Mater. 186, 76 (2011).
[4] L. Ding, C. Wu, H. Deng and X. Zhang, J. Colloid Interface Sci. 376, 224 (2012).
[5] N. Hamdi and E. Srasra, J. Environ. Sci. 24, 617 (2012).
[6] L. Chen, X. L. Chen, C.H. Zhou, H.M. Yang, S.F. Ji, D.S. Tong, Z.K. Zhong, W.H. Yu and M.Q. Chu, J.Cleaner Prod. 156, 648 (2017).
[7] W. Diano, R. Rubino and M. Sergio, Micro. Meso. Mater. 2, 179 (1994).
[8] M.A. De León, C. De Los Santos, L. Latrónica, N.M. Cesio, C. Volzone, J. Castiglioni, M. Sergio, J. Chem. Eng. J. 241, 336 (2014).
[9] L.S. Clesceri, A.E. Greenberg, A.D. Eaton, *Standard Methods for the Examination of Water and Wastewater*, 20th ed. (American Public Health Association, Washington, 1999) p. 246.
[10] K.S.W. Sing, D.H. Everett, R.A.W. Haul, L. Moscou, R.A. Pierotti, J. Rouquerol and T. Siemieniewska, Pure Appl. Chem. 57, 603 (1985).
[11] J. Xu, Y. Li and Y. Xie, Non-Met. Mines 25, 44 (2006).